Onset of multiple sclerosis before adulthood leads to failure of age-expected brain growth

Bérengère Aubert-Broche, PhD
Vladimir Fonov, PhD
Sridar Narayanan, PhD
Douglas L. Arnold, MD
David Araujo, MD, PhD
Dumitru Fetco, MD
Christine Till, PhD
John G. Sled, PhD
Brenda Banwell, MD
D. Louis Collins, PhD
On behalf of the Canadian Pediatric Demyelinating Disease Network

Correspondence to Dr. Banwell: banwellb@email.chop.edu

ABSTRACT

Objective: To determine the impact of pediatric-onset multiple sclerosis (MS) on age-expected brain growth.

Methods: Whole brain and regional volumes of 36 patients with relapsing-remitting MS onset prior to 18 years of age were segmented in 185 longitudinal MRI scans (2–11 scans per participant, 3-month to 2-year scan intervals). MRI scans of 25 age- and sex-matched healthy normal controls (NC) were also acquired at baseline and 2 years later on the same scanner as the MS group. A total of 874 scans from 339 participants from the NIH-funded MRI study of normal brain development acquired at 2-year intervals were used as an age-expected healthy growth reference. All data were analyzed with an automatic image processing pipeline to estimate the volume of brain and brain substructures. Mixed-effect models were built using age, sex, and group as fixed effects.

Results: Significant group and age interactions were found with the adjusted models fitting brain volumes and normalized thalamus volumes ($p < 10^{-4}$). These findings indicate a failure of age-normative brain growth for the MS group, and an even greater failure of thalamic growth. In patients with MS, T2 lesion volume correlated with a greater reduction in age-expected thalamic volume. To exclude any scanner-related influence on our data, we confirmed no significant interaction of group in the adjusted models between the NC and NIH MRI Study of Normal Brain Development groups.

Conclusions: Our results provide evidence that the onset of MS during childhood and adolescence limits age-expected primary brain growth and leads to subsequent brain atrophy, implicating an early onset of the neurodegenerative aspect of MS. ***Neurology*® 2014;83:2140–2146**

GLOSSARY

EDSS = Expanded Disability Status Scale; **FOV** = field of view; **MS** = multiple sclerosis; **NC** = normally developing controls; **NIHPD** = NIH MRI Study of Normal Brain Development; **PDW** = proton density–weighted; **RF** = radiofrequency; **T1W** = T1-weighted; **T2W** = T2-weighted; **TE** = echo time; **TR** = repetition time.

In multiple sclerosis (MS), focal inflammatory white matter lesions are the most visible aspect of pathology but represent only one component of the disease. There is growing evidence that the disease is also characterized by a neurodegenerative component.[1] In adult-onset MS, deep gray matter atrophy is measurable even within the first few years after the first attack.[2]

In cross-sectional analyses, patients with MS with disease onset prior to age 18 years have been shown to have reduced thalamic[3–5] and brain volumes[3,5,6] relative to age- and sex-matched healthy controls. As MS is a chronic progressive illness, and childhood and adolescence are key periods of brain growth,[7] longitudinal analysis is required to define the impact of MS disease on brain development, in order to determine whether these differences in brain volumes are due to failure of normal age-related brain growth or to progressive loss of volume, or both.

In this study, we used longitudinal MRI data to compare the growth trajectory of the brain and specific substructures (thalamus, putamen, caudate, and globus pallidus) in a patient

Editorial, page 2106

Supplemental data at Neurology.org

From the McConnell Brain Imaging Center (B.A.-B., V.F., S.N., D.L.A., D.A., D.F., D.L.C.), Montreal Neurological Institute, McGill University; The Hospital for Sick Children (C.T., J.G.S., B.B.), University of Toronto; York University (C.T.), Toronto, Canada; and Children's Hospital of Philadelphia (B.B.), University of Pennsylvania.

Coinvestigators are listed on the *Neurology*® Web site at Neurology.org.

Go to Neurology.org for full disclosures. Funding information and disclosures deemed relevant by the authors, if any, are provided at the end of the article.

population with MS onset prior to age 18 years to that of a group of age-matched healthy participants. We also investigate the contribution of T2 lesion volumes on brain growth in the patients with MS.

METHODS

Participants. We studied 185 MRI scans of 36 patients (26 female and 10 male) diagnosed with MS (McDonald 2005 criteria[8]) and identified through the Pediatric Demyelinating Disease Clinic at the Hospital for Sick Children. All the patients were required to have been imaged on a single MRI scanner and to have MRI studies that passed the quality control process.

No corticosteroid treatments were received within 1 month of any MRI scan acquisition. The mean age at first scan was 13.77 years (range 5.13–17.72 years) and the mean disease duration (defined from first attack) at first scan was 1.17 years (range 0–4.70 years). Each participant was scanned between 2 and 11 times (mean 5.12 scans), the time between scans varied between 3 months and 2 years, and the follow-up time (time between the first and the last scans) varied between 1.09 and 7.67 years (mean 3.55 years). The mean number of relapses per participant was 3.08 (range 1–10 relapses) and the mean Expanded Disability Status Scale (EDSS) score at the time of the last scan was 1.29 (range 0–3.5). Table e-1 on the *Neurology*® Web site at Neurology.org outlines clinical and follow-up information for each of the patients with MS.

Twenty-five healthy, normally developing controls (the NC group) were recruited (20 female and 5 male; mean age at first scan 16.2 years, range 10.9–22 years). The NC participants were scanned on the same scanner as the MS group on 2 occasions, at intervals of 12–24 months. All NC participants had a negative history for neurologic, medical, or psychiatric illness, learning disability, major head injury, or alcohol or illicit drug abuse.

A total of 874 scans from 339 children from the publicly available NIH-funded MRI Study of Normal Brain Development[9] (termed here the NIH pediatric database or NIH MRI Study of Normal Brain Development [NIHPD] group; 179 female and 160 male; mean age at first scan 11.0 years, range 4.9–19.8 years) were used as the normal growth reference. Participants in the NIHPD study were scanned serially at 2 or 3 time points, with approximately 24 months between scans.

MRI protocol. MRI of the MS and NC participants were obtained using a single GE (Fairfield, CT) 1.5T TwinSpeed Excite 12.0 scanner at the Hospital for Sick Children in Toronto, Canada. The MRI protocol included a whole brain, 3D T1-weighted (T1W) radiofrequency (RF)–spoiled gradient recalled echo sequence (1.5-mm-thick sagittal partitions, repetition time [TR] = 22 msec, echo time [TE] = 8 msec, excitation pulse angle = 30°, field of view [FOV] = 250 mm, 256 × 256 matrix, voxel size = 0.98 × 0.98 × 1.5 mm). To help in lesion segmentation, we acquired a 2D multislice dual-echo proton density–weighted (PDW)/T2-weighted (T2W) fast spin-echo sequence (2-mm-thick slices, no gap, echo train length = 8, TR = 3,500 msec, TE1/TE2 [effective] = 15/63 msec). Scans of the NIHPD controls were obtained at 6 study centers. The MRI protocol included a whole brain, 3D T1W RF-spoiled gradient echo sequence (1-mm-thick sagittal partitions, TR = 22–25 msec, TE = 10–11 msec, excitation pulse angle = 30°, FOV = 160–180 mm). Additional acquisition and participant details are found in Evans et al.[9] The ethics committees of the respective scanning sites approved the study, and informed consent for all participants was obtained from the children's parents or participants old enough to provide informed consent.

Longitudinal image processing. Comprehensive details of the longitudinal processing are described by Aubert-Broche et al.[10] and summarized here.

The preprocessing steps applied to the native T1W images were (1) removing noise,[11] (2) reducing the impact of intensity inhomogeneity,[12] and (3) normalizing the brain volume intensities to the intensities of the target template.[13] For each participant, the preprocessed T1W images of each time point were linearly registered to a participant-specific linear template created using the principles of average template construction described in Fonov et al.[13] For patients with MS, lesions were masked to avoid matching healthy tissue to lesions (the T2W lesion labels[14] were superimposed on the T1W, T2W, and PDW images, carefully reviewed, and, if necessary, manually corrected). A hierarchical 9-parameter linear registration based on an intensity cross-correlation similarity measure was performed between the participant-specific linear template and the ICBM152 template[15] to align the participant-specific template with the population template.

Native T1W images of each visit were resampled once via the concatenated transformation from native space to the participant-specific template space, and from the participant-specific template space to the ICBM152 template space. A multiresolution, nonlocal patch-based segmentation technique was used to extract the brain from the T1W images resampled into the ICBM152 template space, using brain extraction based on nonlocal segmentation technique with a library of priors.[16]

As T1W images of each time point were also registered to a nonlinear participant-specific template that was nonlinearly registered to the population template,[15] the left and right structure (thalamus, putamen, caudate, and globus pallidus) defined on the ICBM152 template were warped back onto each time point's T1W images using the concatenated transformations. For each internal structure, the right and left volumes were combined for analysis.

Brain and internal structure volumes were computed and internal structure volumes were normalized by the brain volume.

All data from the 3 groups (MS, NC, and NIHPD groups) were submitted to the same processing steps defined above: preprocessing, spatial normalization, and volume calculation.

Longitudinal growth analysis. Mixed-effect models were used since it is appropriate to estimate growth in longitudinal studies that take repeated measures from the same individuals over time and it accounts for the within-participant correlation and for varying numbers of measurements for each participant.[17] The coefficients for fixed effects provide estimates of the average response in a group while participant-specific random effects account for heterogeneity among responses from different individuals as well as a covariance pattern among responses within an individual.[18] The models were built using the nlme package[19] in *R* software. Detailed description of the mixed model construction is provided in appendix e-1.

Mixed-effect models were built using MS and NIHPD groups as the NIHPD provided a larger comparator population. To support that the NIPHD could be utilized as a control population, we ensured that there were no scanner-related influences by a mixed-effect analysis that compared our local same-scanner group of NC to the NIHPD group.

We also subdivided the MS group to study the impact of the age at onset or T2 lesion volume on the growth. To study the impact of age at onset, the whole MS group was divided into

2 groups by age at onset (arbitrarily defined as young age <11 years at onset, and older age ≥11 years at onset) and these 2 groups were compared to the NIHPD group. For the second model, we computed a ratio of lesion volume to brain volume for each scan, where the total T2 infratentorial and supratentorial lesion volumes defined the lesion volume. We selected a threshold of 5 cm^3 lesion volume to separate the MS cohort into 2 groups: a minimal lesion volume group and higher lesion volume group. The 5 cm^3 threshold corresponds roughly to a 0.35% lesion-to-brain ratio. Patients who have all scans with a lesion-to-brain ratio less than 0.35% fall into the minimal lesion group, and patients who had one or more scan with the lesion-to-brain ratio greater than 0.35% define the higher-lesion group. These 2 MS groups were compared to the NIHPD group.

RESULTS **Longitudinal analysis.** ***Longitudinal measurements.*** The leftmost graphs in figure 1 represent the measured volumes for the brain and normalized thalamus.

Fitted models. According to the Akaike information criterion values (see appendix e-1 for details), the following quadratic mixed model with fixed and random effects was defined as the best model for brain volume change:

$$\begin{aligned} \mathrm{Vol}_{ij} = {} & \beta_0 + \gamma_{0i} + (\beta_1 + \gamma_{1i})\ \mathrm{Age} + \beta_2.\mathrm{Age}^2 \\ & + \beta_3.\mathrm{Sex}_i + \beta_4.\mathrm{Age} \times \mathrm{Sex}_i \\ & + \beta_5.\mathrm{Age} \times \mathrm{Group}_i + \mathrm{E}_{ij}, \end{aligned}$$

Figure 1 **Brain and normalized thalamus growth trajectories for NIHPD and MS subjects**

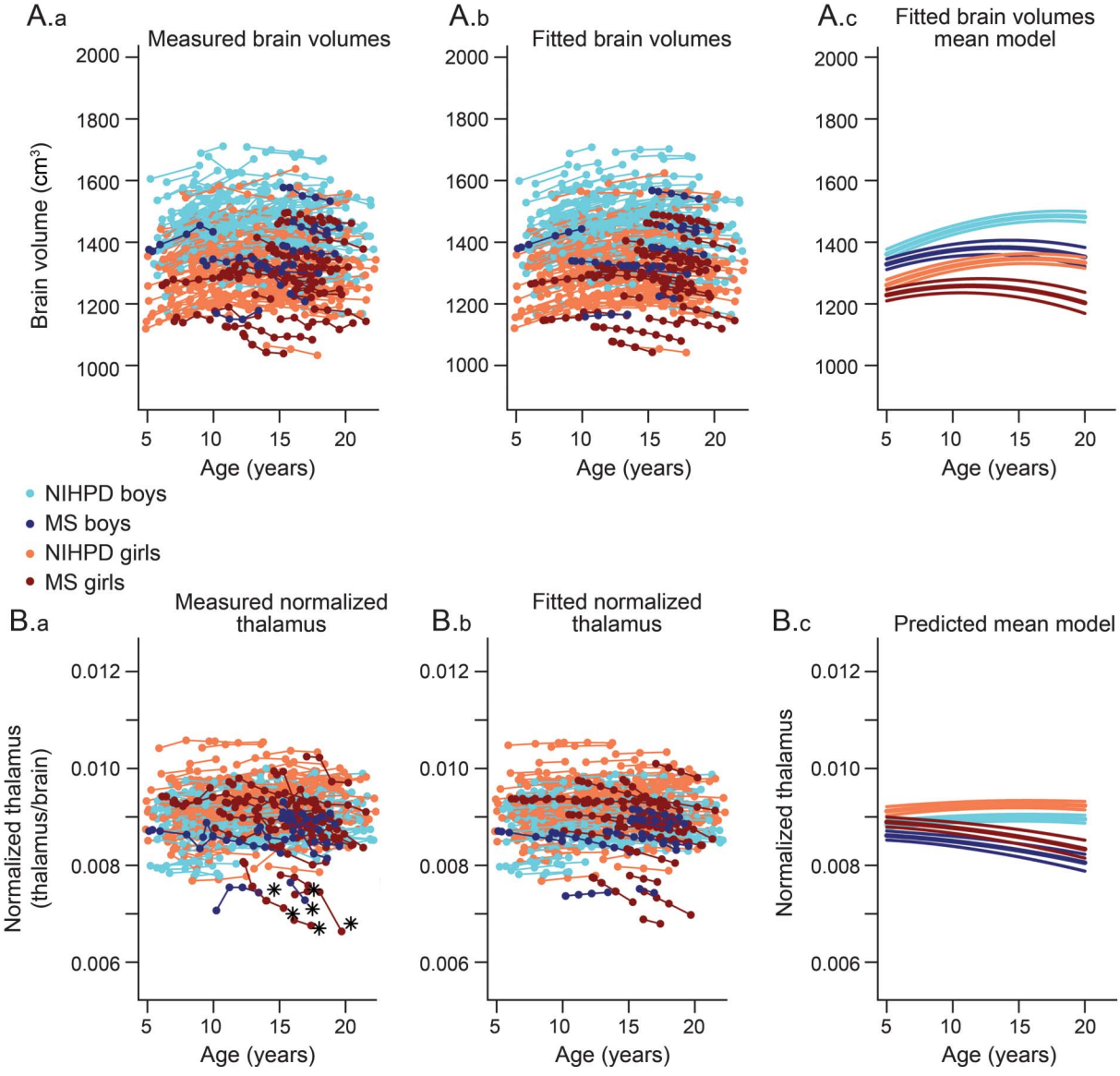

Measured brain volume (Aa), predicted brain volume (Ab), and brain volume mean model with confidence intervals on the mean parameters (Ac) for boys and girls of the NIH MRI Study of Normal Brain Development (NIHPD) and multiple sclerosis (MS) groups. Measured normalized thalamus (Ba), predicted normalized thalamus (Bb), and normalized thalamus mean model with confidence intervals on the mean parameters (Bc) for boys and girls of the NIHPD and MS groups. Note the heterogeneity in the MS group. The participants with an asterisk had a more striking loss of thalamic volume and a more negative slope of thalamic volume over time and were removed from the study (detailed in figure e-1) to determine if they were driving the fit. We found that the resulting parameter values changed only slightly, without changing the statistical results.

where Vol_{ij} is the value of the brain volume for time point j of participant i, β_0 is the intercept, β_1 the linear slope, β_2 the quadratic slope, β_3 the coefficient of sex (multiplied by 1 if male, 0 if female), β_4 the interaction between age and sex, and β_5 the interaction between age and group (multiplied by 0 if NIHPD group, 1 otherwise).

The fixed effect selected variables and obtained values for brain and normalized thalamus models are detailed in table 1. In both models, the age and group interaction coefficients were highly significant ($p < 10^{-4}$) and negative, indicating impaired growth for both brain and normalized thalamus in the MS group compared to the NIHPD group.

From left to right, the top of figure 1 displays individual data points for measured brain volumes, individual data points for predicted brain volumes using the mixed-effects model, and the brain mean models with confidence intervals for the 2 groups. A clear difference in the growth trajectories between male and female participants and between MS and NIHPD groups is demonstrated. The assumption of normality appears reasonable for residuals and both random effects (not shown). The bottom of figure 1 displays the same graphs for normalized thalamic growth, demonstrating a marked difference in the growth trajectories between male and female participants and between MS and NIHPD groups. Note that the difference in thalamic volumes between MS and NIHPD groups has been adjusted for brain size. In figure 2, the mean fitted models for brain volumes (first graph), normalized thalamus (second graph), normalized caudate (third graph), normalized putamen (fourth graph), and normalized globus pallidus (last graph) of MS (top row) and NIHPD groups are presented. As shown in figure 2, growth in brain volume and in normalized thalamic volume is significantly attenuated in the MS group relative to the NIHPD group (top of figure 2, first and second graphs). That is not the case for the normalized caudate and putamen (no significant group and age interaction—top of figure 2, third and fourth graphs). Growth in normalized globus pallidus is significantly attenuated in the MS group relative to the NIHPD group (top of figure 2, fifth graph), although the difference in slope between groups is much smaller than for the normalized thalamus (the graphs have the same range to facilitate comparison between graphs).

As seen in the bottom row of figure 2, when comparing the NC and NIHPD groups, the mean models fitting brain volumes or normalized internal structures do not differ significantly between NC and NIHPD groups (no significant interaction between group and age), indicating that the NC group is representative of the population sampled in the NIH cohort, and that there is no measurable scanner-specific influence.

Impact of age at onset or lesion volumes on growth curves. We selected an arbitrary age threshold of 11 years to investigate the effect of disease onset before or after the start of puberty. The brain or internal structures mean models do not differ significantly between the patients with MS with onset before age 11 years (11 participants, age at first visit 9.88 ± 2.93 years) and the patients with MS with onset after age 11 years (25 participants, age at first visit 15.48 ± 1.65 years).

We selected an arbitrary threshold of 5 cm^3 lesion volume to indicate low lesion volume. For a brain of 1,400 cm^3, 5 cm^3 represents approximately 0.35% of the normalized brain volume. We therefore used 0.35% as a threshold to see the effect of lesion volume on brain atrophy. The brain, normalized caudate, putamen, and globus pallidus mean models do not differ significantly between the patients with MS who have at least one scan with a lesion-to-brain ratio exceeding 0.35% (18 participants, age at first visit 14.81 ± 2.08 years) as compared to patients with MS with low lesion volumes (18 participants, age at

Table 1 Solution for fixed effects for brain model (left) and normalized thalamus (right)

	Mean brain model fixed effects				Mean normalized thalamus model fixed effects			
	Value	Standard error	t Value	$p\ r > \|t\|$	Value	Standard error	t Value	$p\ r > \|t\|$
Intercept (β_0)	1162.62	11.60	100.17	$<10^{-4}$	8.9×10^{-3}	7.2×10^{-5}	124.09	$<10^{-4}$
Age (β_1)	23.36	1.27	18.32	$<10^{-4}$	4.2×10^{-5}	8.8×10^{-6}	4.76	$<10^{-4}$
Age² (β_2)	−0.74	0.04	−16.40	$<10^{-4}$	-1.4×10^{-6}	3.2×10^{-7}	−4.29	$<10^{-4}$
Sex (β_3)	83.84	13.17	6.36	$<10^{-4}$	-2.8×10^{-4}	5.13×10^{-5}	−5.45	$<10^{-4}$
Age × sex (β_4)	3.25	0.69	4.72	$<10^{-4}$	—	—	—	—
Age × group (β_5)	−6.51	0.82	−7.95	$<10^{-4}$	-4.5×10^{-5}	4.7×10^{-6}	−9.53	$<10^{-4}$

$\beta_0 \ldots \beta_5$ are the fixed effects coefficients and are identical for all participants: β_0 is the intercept, β_1 the linear slope, β_2 the quadratic slope, β_3 the coefficient of sex (multiplied by 1 if male, 0 if female), β_4 the interaction between age and sex (multiplied by 1 if male, 0 if female), and β_5 the interaction between age and group (multiplied by 1 if MS group, 0 if NIHPD group).

Figure 2 Estimated mean models

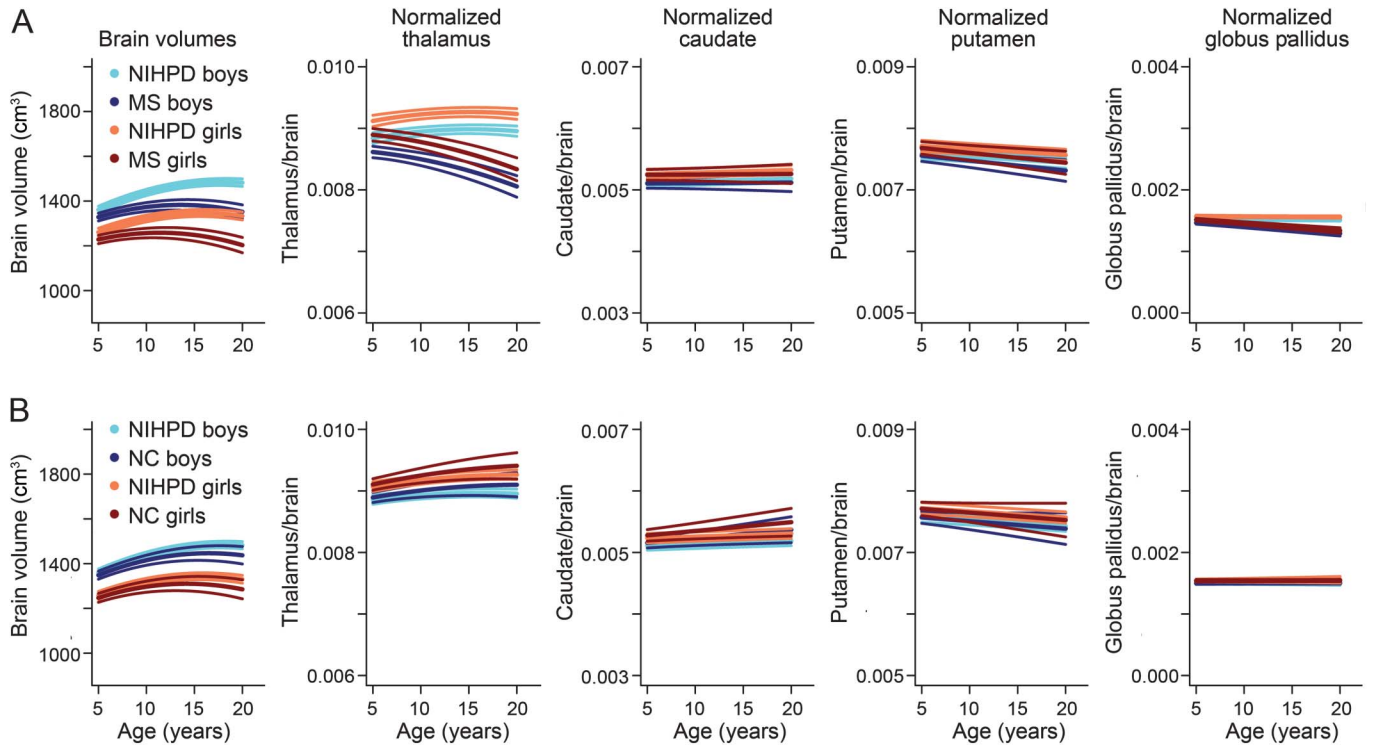

Estimated mean models for NIH MRI Study of Normal Brain Development (NIHPD) and multiple sclerosis (MS) groups (A) and NIHPD and normally developing controls (NC) groups (B). For the normalized brain substructures, each graph has the same range to facilitate the comparison between graphs. The MS and NIHPD models were significantly different only for the brain, thalamus, and globus pallidus. The NC and NIHPD models were not significantly different.

first visit 12.73 ± 4.05 years) (not shown). However, there was a significant group difference between the NIHPD, minimal lesion, and higher lesion volume MS groups in the thalamus longitudinal fitting models (figure 3), where higher lesion load was associated with significantly smaller thalamic volumes over time. When considering lesions within the thalamus specifically, only one participant had a high T2 lesion volume, corresponding to 7% of the size of the thalamus. All other patients with MS had either no T2 lesions visualized in the thalamus or only small thalamic T2 lesion volumes (less than 1.5% of the total thalamic volume).

DISCUSSION We show that the onset of MS during childhood and adolescence impairs age-expected brain growth and leads to abnormally small brain volumes. The brain volumes of our adolescent patients show a progressive loss of volume consistent with brain atrophy. The marked impairment in age-expected growth and the subsequent brain atrophy indicates a clear failure of the anticipated resiliency of the maturing CNS to the brain injury mitigated by MS.

In our prior work, we demonstrated reduced brain volumes in pediatric patients with MS relative to age-expected volume in a cross-sectional analysis.[5] In the present work, we show that the reduced brain volumes demonstrated at a cross-sectional time point are resultant of both a failure of age-expected brain growth as well as a subsequent and progressive reduction in established brain volume (atrophy).

Our findings also confirm prior findings of differences in male and female growth curves in healthy youth,[7] an important issue for future pediatric MS studies, in which brain volume data should be analyzed with consideration of sex.

We analyzed specific brain regions, all of which have been shown in our prior work to be reliably segmented using our methods.[10] Evaluation of the normal control data demonstrates that females have higher thalamic volumes relative to brain size, also an important consideration for future studies, in which sex must be considered in brain volumetric analyses. We then demonstrate a marked difference in thalamic volume normalized by brain size, with both failure of age-expected thalamic growth as well as loss of thalamic volumes. The low normalized thalamus volumes in the MS group compared to the NIHPD indicate that the thalamus is more impacted by the disease than the brain overall. Vulnerability of the thalamus has also been noted in adult-onset MS cohorts, in which loss of volume in the thalamus is one of the earliest and most prominent signs of subcortical gray matter pathology, evident even at the time of a first attack.[20]

Figure 3 Normalized thalamus fitting models with 3 groups

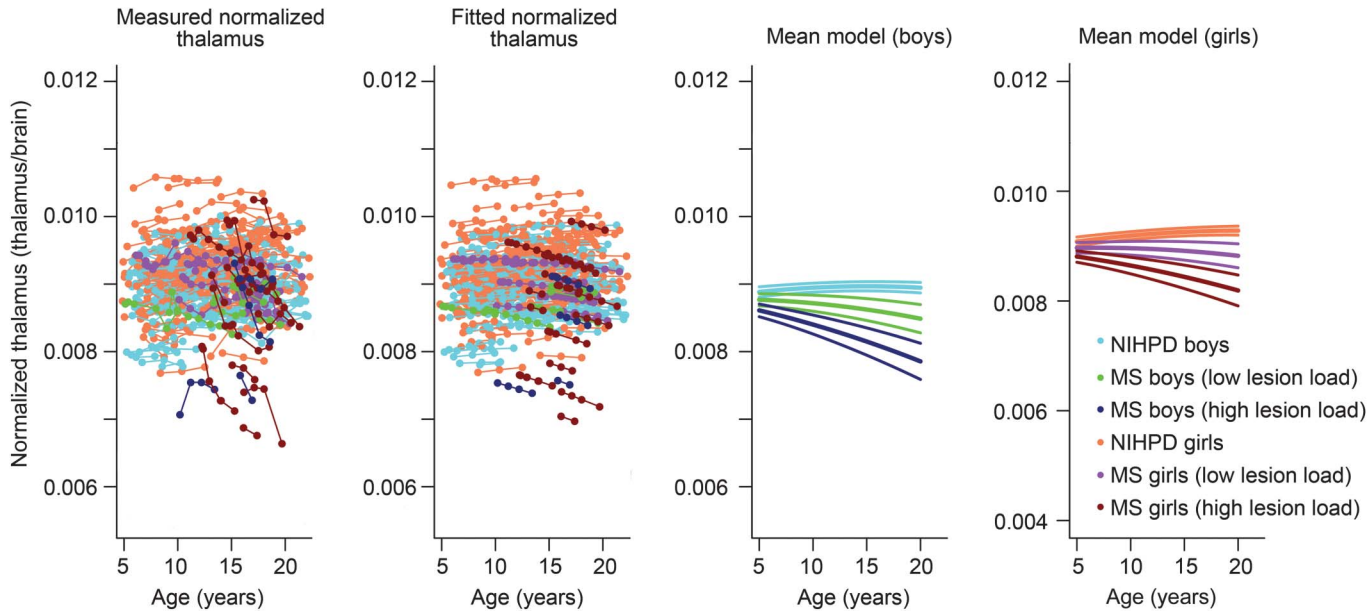

The NIH MRI Study of Normal Brain Development (NIHPD) group, the multiple sclerosis (MS) group with participants who have all scans with the lesion-to-brain ratio inferior to 0.35% (minimal lesion load), and the MS group with participants who have at least one scan with the lesion-to-brain ratio superior to 0.35% (higher lesion load).

When analyzing the data for individual patients, we note that 6 patients with MS (differentiated in figure 1 by an asterisk) seem to have more striking loss of thalamic volume and a more negative slope of thalamic volume over time, indicating rapidly progressive thalamic atrophy. We removed these participants from the model to study how they influence the mean model creation. Without these participants, there was still a significant group difference in thalamic volumes between the MS and NIHPD groups (figure e-1).

The failure of age-appropriate thalamic growth in pediatric- and adolescent-onset MS is even more evident in patients with higher T2 total brain lesion load than in patients with minimal lesion load. However, we noticed that few lesions are detected in the thalamus. Thus, it appears that visible T2 lesions within the thalamus itself are less important for failure of age-appropriate growth than overall disease burden within the brain. Given the role of the thalamus as a relay center in the brain, retrograde and anterograde degeneration of afferent and efferent axons transected in white matter lesions, leading to loss of dendrites and potentially neurons, along with trans-synaptic, activity-dependent loss, may be responsible for the observed failure of age-appropriate thalamic growth. Further studies will be needed to elucidate these findings.

In our prior cross-sectional analysis, a strong correlation was found between cognitive function and reduced size of thalamus and global brain volume,[21] indicative of a functional consequence of reduced brain volume. Future analysis is required to determine whether serial cognitive analyses will demonstrate progressive cognitive decline, and whether the trajectories of cognitive function will mirror the changes in brain volume over time. Of note, physical function was largely intact in our 36 patients, with EDSS scores almost entirely less than 2 throughout the study period, despite frequent relapses (table e-1).

Our data provide compelling evidence that neurodegeneration is an early aspect of MS pathology, rather than a late effect of chronic disease, even in children and adolescents. Such information has import not only to the study of MS pathobiology, but also to considerations for neuroprotection and neurorepair. To date, therapeutic strategies for relapsing-remitting MS have largely focused on the inflammatory biology of the disease, and have been shown to impact relapse frequency. Progressive MS, whether defined by accrual of physical disability in the absence of clear relapses or by progressive evidence of brain injury, is an increasing area of research focus and patient-driven advocacy. Demonstration that such degenerative processes can be measured in patients with MS during childhood and adolescence adds further impetus to consider MS as a degenerative disease from onset and to ensure that future neuroprotective strategies are implemented as early as possible.

AUTHOR CONTRIBUTIONS

Dr. Aubert-Broche conducted the longitudinal MRI analysis and the statistical analysis. Dr. Fonov contributed to the longitudinal MRI analysis. Dr. Collins contributed to the longitudinal MRI analysis and provided

input on the statistical analysis. Dr. Araujo and Dr. Fetco were responsible for producing infratentorial and supratentorial T2 lesion masks. Dr. Till was responsible for participant recruitment, testing, and clinical database development. Dr. Sled and Dr. Narayanan were responsible for the MRI protocol. Dr. Banwell and Dr. Arnold were principal investigators for the Canadian Paediatric Demyelinating Disease Study. All authors contributed to the interpretation of data and the writing and review of the submitted manuscript and have seen and approved the final version.

ACKNOWLEDGMENT

The authors thank Mouiha Abderazzak for his advice on study design and statistical analyses; staff of the Pediatric Demyelinating Disease Program at the Hospital for Sick Children (Toronto, Canada); Julia O'Mahony at the Hospital for Sick Children and Rozie Arnaoutelis at the McConnell Brain Imaging Centre (Montreal, QC, Canada); and the participating children and their families for their cooperation and commitment to our research.

STUDY FUNDING

Supported by the Canadian Institutes of Health Research, the Canadian Multiple Sclerosis Scientific Research Foundation.

DISCLOSURE

B. Aubert-Broche reports no disclosures relevant to the manuscript. V. Fonov has received personal compensation from NeuroRx Research. S. Narayanan has received personal compensation from NeuroRx Research, Teva Neurosciences Canada, and Biogen Idec Canada for consulting services. D. Arnold has served on advisory boards, received speaker honoraria, served as a consultant, or received research support from Bayer, Biogen Idec, Coronado Biosciences, Consortium of Multiple Sclerosis Centers, Eli Lilly, EMD Serono, Genentech, Genzyme, GlaxoSmithKline, MS Forum, NeuroRx Research, Novartis, Opexa Therapeutics, Roche, Merck Serono, S.A. Serono Symposia International Foundation, Teva, the Canadian Institutes of Health Research, and the Multiple Sclerosis Society of Canada; and holds stock in NeuroRx Research. D. Araujo has received personal compensation from NeuroRx Research. D. Fetco, C. Till, and J. Sled report no disclosures relevant to the manuscript. B. Banwell has received speaker's honoraria from Biogen-Idec, Novartis, and Merck-Serono, and serves as an advisor for pediatric trials. None of these activities relate to the present work. D. Collins has received personal compensation from NeuroRx Research and Teva Neurosciences Canada. Go to Neurology.org for full disclosures.

Received February 10, 2014. Accepted in final form July 8, 2014.

REFERENCES

1. Geurts JJ, Calabrese M, Fisher E, Rudick RA. Measurement and clinical effect of grey matter pathology in multiple sclerosis. Lancet Neurol 2012;11:1082–1092.
2. Chard D, Miller D. Grey matter pathology in clinically early multiple sclerosis: evidence from magnetic resonance imaging. J Neurol Sci 2009;282:5–11.
3. Aubert-Broche B, Fonov V, Ghassemi R, et al. Regional brain atrophy in children with multiple sclerosis. NeuroImage 2011;58:409–415.
4. Mesaros S, Rocca MA, Absinta M, et al. Evidence of thalamic gray matter loss in pediatric multiple sclerosis. Neurology 2008;70:1107–1112.
5. Kerbrat A, Aubert-Broche B, Fonov V, et al. Reduced head and brain size for age and disproportionately smaller thalami in child-onset MS. Neurology 2012;78:194–201.
6. Yeh EA, Weinstock-Guttman B, Ramanathan M, et al. Magnetic resonance imaging characteristics of children and adults with paediatric-onset multiple sclerosis. Brain 2009;132:3392–3400.
7. Giedd JN, Blumenthal J, Jeffries NO, et al. Brain development during childhood and adolescence: a longitudinal MRI study. Nat Neurosci 1999;2:861–863.
8. Polman CH, Reingold SC, Edan G, et al. Diagnostic criteria for multiple sclerosis: 2005 revisions to the "McDonald Criteria". Ann Neurol 2005;58:840–846.
9. Evans AC; Brain Development Cooperative Group. The NIH MRI study of normal brain development. NeuroImage 2006;30:184–202.
10. Aubert-Broche B, Fonov VS, Garcia-Lorenzo D, et al. A new method for structural volume analysis of longitudinal brain MRI data and its application in studying the growth trajectories of anatomical brain structures in childhood. NeuroImage 2013;82C:393–402.
11. Coupe P, Manjon JV, Gedamu E, Arnold D, Robles M, Collins DL. Robust Rician noise estimation for MR images. Med Image Anal 2010;14:483–493.
12. Sled JG, Zijdenbos AP, Evans AC. A nonparametric method for automatic correction of intensity nonuniformity in MRI data. IEEE Trans Med Imaging 1998;17:87–97.
13. Fonov V, Evans AC, Botteron K, et al. Unbiased average age-appropriate atlases for pediatric studies. NeuroImage 2011;54:313–327.
14. Francis S. Automatic Lesion Identification in MRI of Multiple Sclerosis Patients. Montreal: McGill University; 2004.
15. Collins DL, Neelin P, Peters TM, Evans AC. Automatic 3D intersubject registration of MR volumetric data in standardized Talairach space. J Comput Assist Tomogr 1994;18:192–205.
16. Eskildsen SF, Coupe P, Fonov V, et al. BEaST: brain extraction based on nonlocal segmentation technique. NeuroImage 2012;59:2362–2373.
17. Bernal-Rusiel JL, Greve DN, Reuter M, Fischl B, Sabuncu MR; for the Alzheimer's Disease Neuroimaging Initiative. Statistical analysis of longitudinal neuroimage data with linear mixed effects models. NeuroImage 2012;66C:249–260.
18. Cheng J, Edwards LJ, Maldonado-Molina MM, Komro KA, Muller KE. Real longitudinal data analysis for real people: building a good enough mixed model. Stat Med 2010;29:504–520.
19. Pinheiro J, Bates D, DebRoy S, Sarkar D, R Core Team. nlme: Linear and Nonlinear Mixed Effects Models. R package version 3.1-104; 2009. Available at: http://CRAN.R-project.org/package=nlme.
20. Minagar A, Barnett MH, Benedict RH, et al. The thalamus and multiple sclerosis: modern views on pathologic, imaging, and clinical aspects. Neurology 2013;80:210–219.
21. Till C, Ghassemi R, Aubert-Broche B, et al. MRI correlates of cognitive impairment in childhood-onset multiple sclerosis. Neuropsychology 2011;25:319–332.